

Molecular Docking and 3D-QSAR CoMFA Studies on Indole Inhibitors of GIIA Secreted Phospholipase A₂

Varnavas D. Mouchlis, Thomas M. Mavromoustakos,* and George Kokotos

Laboratory of Organic Chemistry, Department of Chemistry, University of Athens, Panepistimiopolis, Athens 15771, Greece

Received June 2, 2010

Automated docking allowing a “protein-based” alignment was performed on a set of indole inhibitors of the GIIA secreted phospholipase A₂ (GIIA sPLA₂). A correlation between the binding scores and the experimental inhibitory activity was observed ($r^2 = 0.666$, $N = 34$). All the indole inhibitors were docked in the active site of the GIIA sPLA₂ enzyme, and the best score docking pose of each inhibitor was used for the “protein-based” alignment of the compounds. A three-dimensional quantitative structure–activity relationship (3D-QSAR) model was then established using the comparative molecular field analysis (CoMFA) method. The set of 34 indole inhibitors was divided into two subsets: the training set, composed of 26 compounds, and the test set, consisting of eight compounds. The robustness and the predictive ability of the generated CoMFA model were examined by using the test set. A good correlation ($r^2 = 0.997$) between predicted and experimental inhibitory activity data allows the validation of the CoMFA model. Finally, the generated CoMFA model was used for the design and evaluation of new compounds. The new designed compounds exert improved predicted inhibitory activity and may be a target for the synthesis of new GIIA sPLA₂ indole inhibitors.

1. INTRODUCTION

Phospholipase A₂ corresponds to a superfamily of enzymes that to date include 15 separate, identifiable groups and numerous subgroups of PLA₂ enzymes.^{1,2} These enzymes catalyze the hydrolysis of the ester bond of membrane phospholipids at the *sn*-2 position. The five main categories of PLA₂ enzymes are: the secreted sPLA₂s, the cytosolic cPLA₂s, the Ca²⁺-independent iPLA₂s, the PAF acetylhydrolases, and the lysosomal PLA₂s.

The products of the *sn*-2 ester bond hydrolysis of phospholipids by the PLA₂ enzymes are free fatty acids and lysophospholipids. The action of the PLA₂ enzymes on the phospholipids is of high importance when the esterified fatty acid at the *sn*-2 position is arachidonic acid (AA). AA is converted by different downstream metabolic enzymes (such as COX-1, COX-2 and 5-LO) to several bioactive lipid mediators called eicosanoids, including prostaglandins (PGs) and leukotrienes (LTs).^{3,4} The eicosanoids participate in many pathological inflammatory conditions, such as atherosclerosis⁵ and ischemia diseases.⁶ The lysophospholipids are precursors of other bioactive mediators, such as the platelet activating factor (PAF).⁷

PLA₂ enzymes are membrane-bound enzymes, and as a result they have an *i*-face that has been proposed to make contact with the substrate interface.⁸ The *i*-face of the sPLA₂ enzymes is a relatively flat surface of 1600 Å², which binds tightly to the phospholipid bilayers ($K_d < 10^{-13}$ M).⁹ There are some polar and hydrophobic residues on the flat surface, through which the sPLA₂s bind to the ionic bilayers. The

sPLA₂ enzymes are interfacial enzymes, and their active site is localized near the substrate binding *i*-face.¹⁰

There are 10 known members of sPLA₂ enzymes that have been identified in mammals, which are numbered and classified in groups according to the chronological order of their discovery. The 10 groups of the sPLA₂ enzymes are: IB, IIA, IIC–F, III, V, X, and XII.¹¹ The characterization of their molecular structure, the classification, the genome localization, and the details of their catalytic mechanism attracted the research interest of many scientists.^{11–15} In the class of the low molecular weight secreted PLA₂ enzymes, the group IIA secreted PLA₂ (GIIA sPLA₂) is of paramount importance since it is involved in several inflammatory diseases, such as rheumatoid arthritis, and was cloned in 1989.^{16,17} In vitro studies using recombinant GIIA sPLA₂ on phospholipid substrates have provided important information about the biochemistry of the enzyme. For instance, the GIIA sPLA₂ (known as human nonpancreatic sPLA₂) shows biological activity on ionic phospholipids, such as phosphatidylglycerol (PG), phosphatidylserine (PS), and phosphatidylethanolamine (PE), but it is inactive on phosphatidylcholine (PC).¹⁸

GIIA sPLA₂ is a disulfide-linked enzyme, with seven disulfide bonds, which contribute to the folding and stability of the enzyme structure. In addition, it has a Ca²⁺-binding loop and a His/Asp catalytic dyad. The mechanism of substrate hydrolysis begins by the activation of a water molecule by the catalytic histidine (His47). Beside this histidine, there is an aspartate residue (Asp48), which together with three other residues (Gly29, Gly31, and His27) construct the conserved Ca²⁺-binding loop, where the Ca²⁺ ion is bound.¹⁹ The hepta-coordinated Ca²⁺ ion provides two positions for the substrate binding, one axial and one

* Corresponding author. E-mail: tmavrom@chem.uoa.gr. Telephone: +30 2107274293.

equatorial.²⁰ The high-resolution crystal structures of the GIIA sPLA₂ enzyme have defined an enclosed active site with a hydrophobic region which is located near the N-terminal helix.^{21,22} This hydrophobic region contributes to the binding of a phospholipid molecule and to the interfacial binding of the enzyme to the phospholipid bilayers.

The GIIA sPLA₂ enzyme is an attractive target for the development of new inhibitors, which might lead to therapeutic drugs for diseases where the enzyme is involved. It has also been crystallized with or without different ligands, and this fact renders the enzyme a suitable target for drug design using computational methods.^{23–28} Many different classes of synthetic and natural inhibitors are known to date.^{29–33} However, in order to enhance the design of new GIIA sPLA₂ inhibitors, the requirements are: (i) the knowledge of the exact location of the active site and the understanding of the inhibitor–enzyme interactions; and (ii) the establishment of drug design computational protocols to predict the activity of new designed molecules.

The main computational methods used in the rational drug design can be divided into two groups: (i) protein-based studies, which include molecular docking studies^{23,24} and molecular dynamics simulations^{25,26} (MD) (wherein the receptor–ligand interactions model is simulated); and (ii) quantitative structure–activity relationship (QSAR) analysis,^{27,28} which does not require a priori hypothesis about the receptor structure. The QSAR analysis is based on the pharmacophore alignment of the ligands and implies a common biochemical mechanism.

Molecular docking is an extensively used computational method in rational drug design,³⁴ and the main principals that govern this technique have been described in recent review articles.^{35–37} For any docked pose, the binding score is calculated generally as the sum of the electrostatic, van der Waals and hydrophobic interactions, and hydrogen bonding. Some scoring functions include also metal-binding and solvation terms. Methodologies have been developed to pick up the pose that simulates best the biological molecular interactions.³⁸

The 3D-QSAR comparative molecular fields analysis (CoMFA)³⁹ requires the alignment of all the studied molecules in a three-dimensional space. In conventional CoMFA studies, the molecules are fitted to a reference molecule, which is the most rigid or constrained molecular structure among the most active compounds. The hypothesis in this case is that the conformation of the reference compound is supposed to correspond to the “biologically active” conformation. In the case of a known X-ray crystal structure with high resolution, a structure-based design protocol reduces the uncertainty about the determination of the “bioactive conformation” of the reference compound. A protocol of automated molecular docking of all the available compounds in the receptor active site creates an indubitable “receptor-based” alignment for the CoMFA analysis.

The present study is consisted of molecular docking calculations and the generation of a CoMFA model on a set of GIIA sPLA₂ indole inhibitors reported in the literature.⁴⁰ All the GIIA sPLA₂ indole inhibitors were docked in the enzyme active site using GLIDE 5.5.^{41–43} The extra-precision⁴⁴ (XP) mode of GLIDE was used for the docking calculations. The best score docking pose of each indole

inhibitor was used in a “protein-based” alignment for the CoMFA procedure. The quality of the CoMFA analysis depends greatly on the alignment of the studied compounds. “Protein-based” alignment via molecular docking allows the development of a high-quality CoMFA model.

2. COMPUTATIONAL METHODS

2.1. Preparation of the GIIA sPLA₂ Enzyme File. Four crystal structures of the GIIA sPLA₂ enzyme which are deposited in the RCSB protein data bank were downloaded (PDB IDs: 1DB4 holo form 2.20 Å X-ray resolution,⁴⁵ 1DB5 holo form 2.80 Å X-ray resolution,⁴⁵ 1KVO holo form 2.00 Å X-ray resolution,⁴⁶ and 1J1A holo form 2.20 Å X-ray resolution⁴⁷). The objective was to judge which one is sufficient for docking the indole inhibitors. The procedure for this determination is consisted by the following steps: (i) using “superposition panel” of Maestro 9.0⁴⁸ all the crystal structures were superimposed based on all the backbone atoms including beta carbons. The crystal structure with PDB ID: 1DB4 was chosen as the reference structure for the superposition (rmsd between: 1DB4–1DB5: 0.147 Å, 1DB4–1J1A: 0.746 Å, 1DB4–1KVO: 0.487 Å). No significant structural differences were observed (see Figure 1 in Supporting Information); (ii) the active site region was examined to determine if the superimposed ligands can fit into the reference site without steric clashes. No significant steric clashes were observed; (iii) the active site region of all the crystal structures, in turn, was examined in order to determine whether any residues in the superimposed protein differ appreciably in position or conformation from those in the reference site. No significant differences were observed. Thus, the 1DB4.pdb file has been chosen for the molecular docking calculations. This file contains a single unit of the GIIA sPLA₂ enzyme cocrystallized with a native indole inhibitor, which is structurally similar with the indole inhibitors used in this study. The 1DB4.pdb crystal structure was prepared using the “Protein Preparation Wizard” panel⁴⁹ of Schrödinger 2009 molecular modeling package. In particular, using the “preprocess and analyze structure” tool, the bond orders were assigned, all the hydrogen atoms were added, the calcium ion was treated in order to have the correct geometry and formal charge (+2), the disulfide bonds were assigned, and all the water molecules in a distance greater than 5 Å from any heterogroup were deleted. Using Epik 2.0,^{50,51} a prediction of the heterogroups ionization and tautomeric states was performed. An optimization of the hydrogen-bonding network was performed using the “H-bond assignment” tool. Finally, using the “impref utility”, the positions of the hydrogen atoms were optimized by keeping all the heavy atoms in place.

2.2. Preparation of Ligands Files. All the indole ligands were built and adjusted using the Maestro 9.0 molecular builder. All the hydrogen atoms were added, and the ligands were submitted in full structure optimization, using the minimization procedure of MacroModel 9.7.⁵² For the minimization, a standard molecular mechanics energy function (OPLS_2005⁵³ force field) and the Polak–Ribiere conjugated gradient method (5000 iterations with gradient 0.01 kJ/mol·Å)⁵⁴ were used. Solvent effects were modeled with the generalized Born/surface area (GB/SA) implicit solvent model⁵⁵ using water as solvent and normal non-

bonded cutoffs. The constant dielectric electrostatic treatment was selected with a dielectric constant of 1. The minimized structures of the indole ligands were subsequently prepared using LigPrep 2.3.⁵⁶ In particular, using LigPrep 2.3 all the structures were checked to be correct, ionization states were generated for all the indole inhibitors by taking into account the metal mode of Epik 2.0 ionizer for the metalloproteins, and the OPLS_2005 force field was used for the structure optimization of all the indole ligands.

2.3. Receptor Grid Generation for the GIIA sPLA₂ Enzyme. Glide is a grid-based ligand docking with energetics approach and searches for favorable interactions between ligands and receptors. The shape and properties of the receptor are represented on a grid by different sets of fields that provide progressively more accurate scoring of the ligand pose (by “pose” we mean a complete specification of the ligand: position and orientation relative to the receptor, core conformation, and rotamer-group conformations). These fields are generated as preprocessing steps in the calculation and hence need to be computed only once for each receptor. For the grid generation of the GIIA sPLA₂ enzyme, the binding site was defined using the native indole ligand cocrystallized with the enzyme. The default value (1.00) for the van der Waals radii scaling factor was chosen, which means no scaling for the nonpolar atoms was performed (no flexibility was simulated for the receptor). Glide uses two boxes to organize the calculation: (i) the grids are calculated within the space defined by the enclosed or outer box. This is also the box in which all the ligand atoms must be contained; (ii) acceptable positions for the ligand center during the site point search lie within the ligand diameter midpoint box or the inner box. This box gives a more precise measure of the effective size of the search space. However, ligands can move outside this box during grid minimization. The native indole inhibitor has a very similar size with the indole ligands of this study, and for defining the size of the inner box, the option “docking ligands similar in size to the workspace ligand” was chosen. The Cartesian coordinates of the inner box, X, Y, and Z length were set to 12 Å.

2.4. Protocol of Grid-Based Ligand Docking with Energetics (Glide). Glide uses a series of hierarchical filters to search for possible locations of the ligand in the active site region of the receptor. For the grid-based ligand docking with energetics, the receptor grid generation file was used (see Section 2.3). The next step is to define the conformational space of the ligand. Glide uses a sophisticated fashion described by Friesner and co-workers to choose six lowest-energy poses.⁴² Finally, the three to six lowest-energy poses obtained in this fashion are subjected to a Monte Carlo procedure that examines nearby torsional minima. This procedure is needed in some cases to properly orient peripheral groups and occasionally alters internal torsion angles. To soften the potential for nonpolar parts of the ligands the “scaling of van der Waals radii” was used with “scaling factor” of 0.8 and “partial charge cutoff” of 0.15. Glide uses the GlideScore in order to rank poses. GlideScore is a modified and expanded version of ChemScore⁵⁷ scoring function that is used for predicting binding affinity and rank-ordering ligands in database screens. By using GlideScore as the scoring function, a composite Emodel score is then used to rank the poses of each ligand and to select the poses to be reported to the user. Emodel combines GlideScore, the

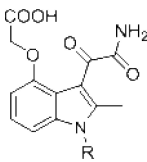
nonbonded interaction energy, and for flexible docking, the excess internal energy of the generated ligand conformation. In the present study the extra-precision⁴⁴ (XP) mode of GlideScore scoring function was used. XP mode can be used when the active site of the receptor contains a metal and often works well. Glide assigns a special stability to ligands in which anions coordinate to the metal center. To benefit from this assignment, groups such as carboxylates, hydroxamates, and thiolates must be anionic. The protein residues that line the approach to the metal center need to be protonated in a manner compatible with the coordination of an anionic ligand, such as a carboxylate or hydroxamates. With respect to the GIIA sPLA₂ enzyme, the calcium ion has charge of +2, but the effective charge which GLIDE uses to dock the ligands is +1 because the ionic carboxylate group of Asp48, that bears a charge −1, binds to the calcium ion. The GlideScore XP scoring function also includes terms which assign penalties to structures where statistical results indicate that one or more groups is inadequately solvated. A large database of cocrystallized structures has been used by the creators of the scoring function, to optimize the parameters associated with the penalty terms. No penalties on the docked structures were observed. The force field used for the docking was the OPLS_2001.

2.5. CoMFA. **2.5.1. Data Set (Training and Test Sets).** The 34 indole inhibitors and the corresponding biological data used in this study have been selected from the literature.⁴⁰ The molecular structures and the GIIA sPLA₂ inhibitory activity data for these 34 indole inhibitors are summarized in Table 1. All the collected biological data (% inhibition) were measured in vitro under the same experimental conditions.⁴⁰

These 34 compounds were divided into two subsets: 26 of them were used as a training set, and 8 were used as a test set. The compounds were separated to training and test sets in order for the two sets to have a good molecular diversity. Both, training and test sets included active and inactive compounds to a scale from 0 to 100% inhibition against the GIIA sPLA₂ enzyme.

2.5.2. Data Set Alignment. In the 3D-QSAR CoMFA analysis, biological conformation and alignment rule selection are two important factors to construct a reliable model. In the present study, the poses from the automated molecular docking calculations by GLIDE were used for the alignment method. Compound **1** was selected as a template molecule for the alignment. Considering the structural similarities of the studied indole inhibitors, 17 common atoms of compounds **1–34** were selected for the alignment. The alignment of the molecules was performed using the module “database alignment” in SYBYL 8.0 molecular modeling package. The alignment results are shown in Figure 2 in the Supporting Information with the common atoms highlighted in magenta color in compound **1**.

2.5.3. CoMFA Analysis. In the present study, a “protein-based” alignment was used (the conformations of the studied compounds used for the alignment were chosen by docking these compounds in the GIIA sPLA₂ enzyme active site). Atomic charges for the aligned molecules were calculated using the Gasteiger–Hückel method, which is a combination of two other charge computational methods: the Gasteiger–Marsili⁵⁸ method to calculate the σ component of the atomic charge and the Hückel⁵⁹ method to calculate the π compo-

Table 1. In Vitro % Inhibition of the Indole Inhibitors⁴⁰ Against the GIIA sPLA₂ Enzyme and the XP Binding Scores Calculated by GLIDE


compound	R group	% inhibition against GIIA sPLA ₂	XP GScore
Training Set			
1	2,6-Cl ₂ -C ₆ H ₃ CH ₂	100	-11.21
2	3-I-C ₆ H ₄ CH ₂	98	-10.45
3	3-(OCF ₃)-C ₆ H ₄ CH ₂	97	-10.45
4	3-Cl-C ₆ H ₄ CH ₂	96	-10.61
5	3-Br-C ₆ H ₄ CH ₂	95	-10.29
6	2-(CF ₃)-C ₆ H ₄ CH ₂	93	-10.68
7	2,6-F ₂ -C ₆ H ₃ CH ₂	91	-10.73
8	CH ₃ (CH ₂) ₆	89	-9.70
9	4-(CH ₃)-C ₆ H ₄ CH ₂	88	-10.41
10	3-CN-C ₆ H ₄ CH ₂	86	-10.47
11	2,4-F ₂ -C ₆ H ₃ CH ₂	84	-10.69
12	4-(CF ₃)-C ₆ H ₄ CH ₂	83	-9.71
13	C ₆ H ₅ CH ₂	82	-10.72
14	4-F-C ₆ H ₄ CH ₂	80	-10.59
15	CH ₃ (CH ₂) ₅	79	-9.96
16	2,5-F ₂ -C ₆ H ₃ CH ₂	76	-10.63
17	(CH ₃) ₂ CHCH ₂	64	-9.76
18	C ₆ H ₅ COCH ₂	61	-9.41
19	3-(NO ₂)-C ₆ H ₄ CH ₂	57	-9.78
20	CH ₃ (CH ₂) ₂	51	-9.32
21	CH ₃ CH ₂	39	-9.17
22	4-CN-C ₆ H ₄ CH ₂	29	-9.74
23	1-(8-CH ₂ Br)-naphthaleneCH ₂	24	-9.18
24	4-(7-CH ₃ O)-coumarinylCH ₂	9	-9.97
25	2-(OCH ₃)-5-(NO ₂)-C ₆ H ₃ CH ₂	7	-8.85
26	phthalimidoCH ₂	0	-6.48
Test Set			
27	2-naphthaleneCH ₂	97	-10.82
28	2-(CF ₃)-4-F-C ₆ H ₃ CH ₂	93	-10.46
29	3-(CH ₂ Br)-C ₆ H ₄ CH ₂	86	-10.64
30	CH ₃ (CH ₂) ₃	69	-9.90
31	CH ₃ (CH ₂) ₄	57	-9.48
32	C ₆ F ₅ CH ₂	33	-9.38
33	(S)-(+)-CH ₃ CH ₂ CH(CH ₃)CH ₂	22	-8.97
34	phthalimido(CH ₂) ₄	2	-8.63

nent of the atomic charge. The total charge is the sum of the charges calculated by the two methods. The CoMFA fields are generated by creating a grid around the molecule and calculating the steric and electrostatic potentials at each point on the grid using a charged probe atom. The CoMFA calculations were performed using Tripos Advance CoMFA⁶⁰ module in SYBYL 8.0. The steric and electrostatic field energies were calculated using the Lennard-Jones and coulomb potentials, respectively with $1/r^2$ distance-dependent dielectric constant in all intersections of regularly spaced (0.2 nm) grid. The sp³ carbon atom with radius of 1.53 Å and charge +1.0 was used as a probe to calculate the steric and electrostatic energies between the probe and the molecules using the standard Tripos force field.⁶¹ The truncation for both the steric and electrostatic energies was set to 30 kcal mol⁻¹. This indicates that any steric or electrostatic field value that exceeds this value will be replaced with 30 kcal mol⁻¹, thus makes a plateau of the fields close to the center of any atom.

2.5.4. Partial Least-Squares (PLS) Analysis and Validations. The initial PLS analysis is used to correlate the experimental inhibitory activity of the indole inhibitors against the GIIA sPLA₂ enzyme with the CoMFA values containing magnitude of steric and electrostatic potentials. CoMFA standard scaling was applied to all the CoMFA analysis. The full PLS analysis was run with a column filtering of 2.0 kcal mol⁻¹ to reduce the noise and to speed up the calculation. In CoMFA analysis, descriptors were treated as independent variables, whereas the % inhibition against the GIIA sPLA₂ enzyme values were treated as dependent variables in the PLS regression analyses to derive the 3D-QSAR model. The model was assessed by their cross-validated r^2 (r^2_{cv}) using leave-one-out (LOO) procedure.^{62,63} The final model (non-cross-validated conventional analysis) was developed from the model with the highest cross-validated r^2 (r^2_{cv}). The non-cross-validated model was assessed by the r^2 conventional correlation coefficient, the s standard error of prediction, and the F value (Fisher test).

To obtain confidence limits and test the stability of obtained PLS model, for the conventional CoMFA run, bootstrapping⁶⁴ was performed (100 runs, column filtering: 2.00 kcal mol⁻¹). The idea is to simulate a statistical sampling procedure by assuming that the original data set is the true population and generating many new data sets from it. These new data sets (called bootstrap samplings) are of the same size as the original data set and are obtained by randomly choosing samples (rows) from the original data, with repeated selection of the same row being allowed. The statistical calculation is performed on each of these bootstrap samplings, with new values being calculated for each of the parameters to be estimated. The difference between the parameters calculated from the original data set and the average of the parameters calculated from the many bootstrap samplings is a measure of the bias of the original calculation.⁶⁰

3. RESULTS AND DISCUSSION

3.1. Molecular Docking Results. In this section, the results derived from the docking of the indole inhibitors in the GIIA sPLA₂ enzyme active site will be discussed. The attention has been focused on the most characteristic receptor–ligand interactions for a few key inhibitor structures and especially for compound **1**, the most active one in the data set.

The established automated molecular docking was first applied to two indole inhibitors already cocrystallized with the GIIA sPLA₂ enzyme and described by Schevitz et al.⁴⁵ These two compounds (see Table 1 in the Supporting Information) are structurally very similar to the indole inhibitors in this study. By docking these compounds, it was possible to examine if GLIDE is able to reproduce crystallographic experimental data for structural similar compounds. Afterward, the 34 indole inhibitors in this study were docked in the GIIA sPLA₂ enzyme active site, and the inhibitory activity was compared with the XP binding scores calculated by GLIDE. The purpose of this docking was to examine if there is a correlation between the experimental % inhibitory activity and the theoretical XP binding scores.

The crystallographic data reveal the following interactions of indole8⁴⁵ and indole6⁴⁵ with the GIIA sPLA₂ enzyme

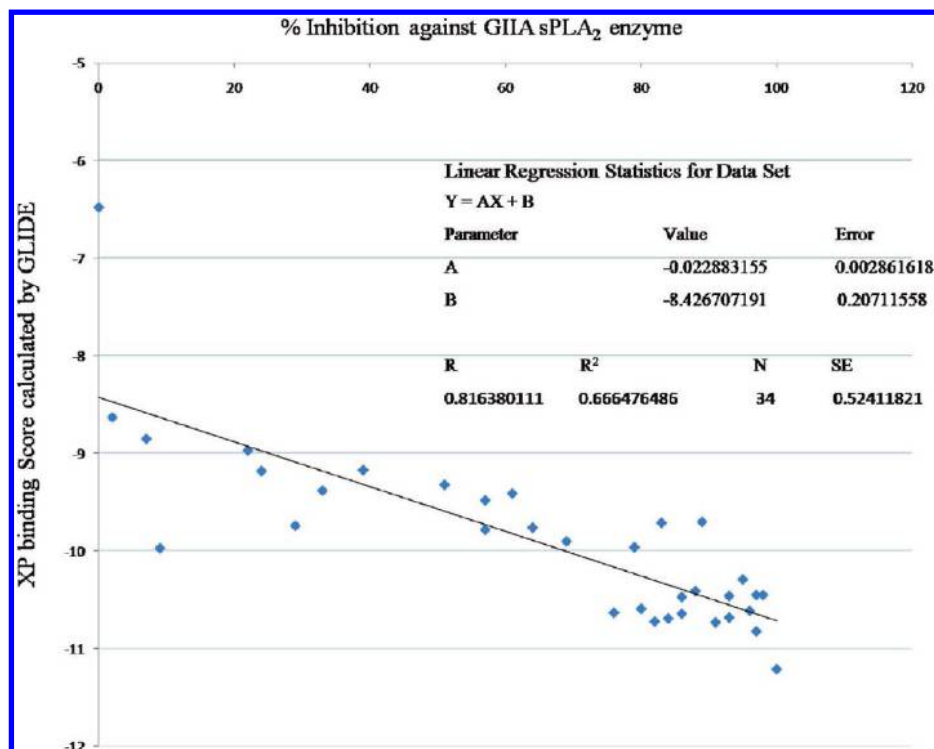


Figure 1. Plot of the experimental % inhibition against the GIIA sPLA₂ enzyme versus the XP binding scores calculated by GLIDE. The linear regression statistics for the data set are also presented.

active site: (i) two interactions between two oxygen atoms of the ligands and the calcium ion and (ii) one hydrogen bond with His47. In the case of indole8, one oxygen atom of the phosphonate group participates in a hydrogen bond with Lys62 through a water molecule placed near the enzyme active site. The compounds indole8 and indole6 were docked successfully by GLIDE. The interactions aforementioned were reproduced, and the conformation of each ligand was almost identical to the crystallographic one. In addition, three other hydrogen bonds were observed between one hydrogen atom of the amide group and Asp48, the oxygen atom of the amide group and Gly29 and one of the oxygen atoms of the carboxylate or phosphonate group with Gly31 (see Figure 3 and Table 1 in the Supporting Information).

The docking calculations were then applied to the 34 indole inhibitors in this study. The computed XP binding scores of the indole inhibitors from the docking calculations with GLIDE were compared with their experimental inhibitory activity against the GIIA sPLA₂ enzyme (Table 1). The linearity of the plot ($r^2 = 0.666$, $N = 34$) presents a good correlation between the XP binding scores and the inhibitory activity of the indole inhibitors (Figure 1).

In Figure 2 the binding of the most active compound **1** is presented and reveals the main interactions with the enzyme active site. The observed interactions are: (i) two interactions of two oxygen atoms (the oxygen atom of the amide group and one of the oxygen atoms of the carboxylate group) with the calcium ion ($\text{COO}^- \cdots \text{Ca}^{2+}$ 2.30 and $\text{NHCO} \cdots \text{Ca}^{2+}$ 2.70 Å); (ii) one hydrogen bond of one of the hydrogen atoms of the amide group with the nitrogen atom of His47 ($\text{H} \cdots \text{N}$, 1.90 and $\text{N} \cdots \text{N}$ 2.90 Å); (iii) one hydrogen bond of one of the hydrogen atoms of the amide group with the oxygen atom of Asp48 ($\text{H} \cdots \text{O}$ 1.80 and $\text{O} \cdots \text{O}$ 2.70 Å); (iv) one hydrogen bond of the oxygen atom of the amide group with the hydrogen atom of the amine group of Gly29 ($\text{O} \cdots \text{H-N}$ 2.10

and $\text{O} \cdots \text{N}$ 2.80 Å); and (v) one hydrogen bond of one of the oxygen atoms of the carboxylate group with the hydrogen atom of the amine group of Lys62 through a water molecule placed near the active site of the enzyme ($\text{O} \cdots \text{H}-\text{O} \cdots \text{H}-\text{N}$ 2.50, 1.90 and $\text{O} \cdots \text{O} \cdots \text{N}$ 3.00, 2.90 Å). The phenyl ring of compound **1** participates in aromatic ($\pi-\pi$) stacking interactions with the residues Phe5 ($R_{\text{cen}} = 6.49$ Å, $\theta = 9.40^\circ$) and His6 ($R_{\text{cen}} = 5.76$ Å, $\theta = 70.77^\circ$), and the indole ring participates also in aromatic ($\pi-\pi$) stacking interactions with Phe5 ($R_{\text{cen}} = 5.88$ Å, $\theta = 84.86^\circ$) and His47 ($R_{\text{cen}} = 6.64$ Å, $\theta = 70.20^\circ$). Aromatic ($\pi-\pi$) stacking interactions are one of the forces governing molecular recognition. Burley and Petsko have reported that aromatic ($\pi-\pi$) stacking interactions in proteins operate at distances (R_{cen}) of 4.5–7.0 Å between the center mass of the rings, the rings' centroids.⁶⁵ The angle (θ) between normal vectors of interacting aromatic rings is typically between 30° and 90° , producing a “tilted-T” or “edge-to-face” arrangement of interacting rings. Hunter and co-workers⁶⁶ have reported that aromatic ($\pi-\pi$) parallel stacking interactions ($\theta < 30^\circ$) between phenylalanine residues in proteins are also favorable, if the rings are offset from each other. The two chlorine atoms participate in van der Waals contacts with the carbon atoms of the site chains of Phe5, Ile9, Ala17, Ala18, and Tyr21.

In the 34 indole inhibitors described in this study, the main structural changes are in the R group. This position is governed mainly by steric effects in the active site of the GIIA sPLA₂ enzyme. In Figure 3 the binding of the inactive compound **25** is presented. The main interactions of compound **25** in the active site of the enzyme are: (i) two interactions of the two oxygen atoms (the oxygen atom of the amide group and one of the oxygen atoms of the carboxylate group) with the calcium ion ($\text{COO}^- \cdots \text{Ca}^{2+}$ 2.30 and $\text{NHCO} \cdots \text{Ca}^{2+}$ 2.60 Å); (ii) one hydrogen bond of one of the hydrogen atoms of the amide group with the nitrogen

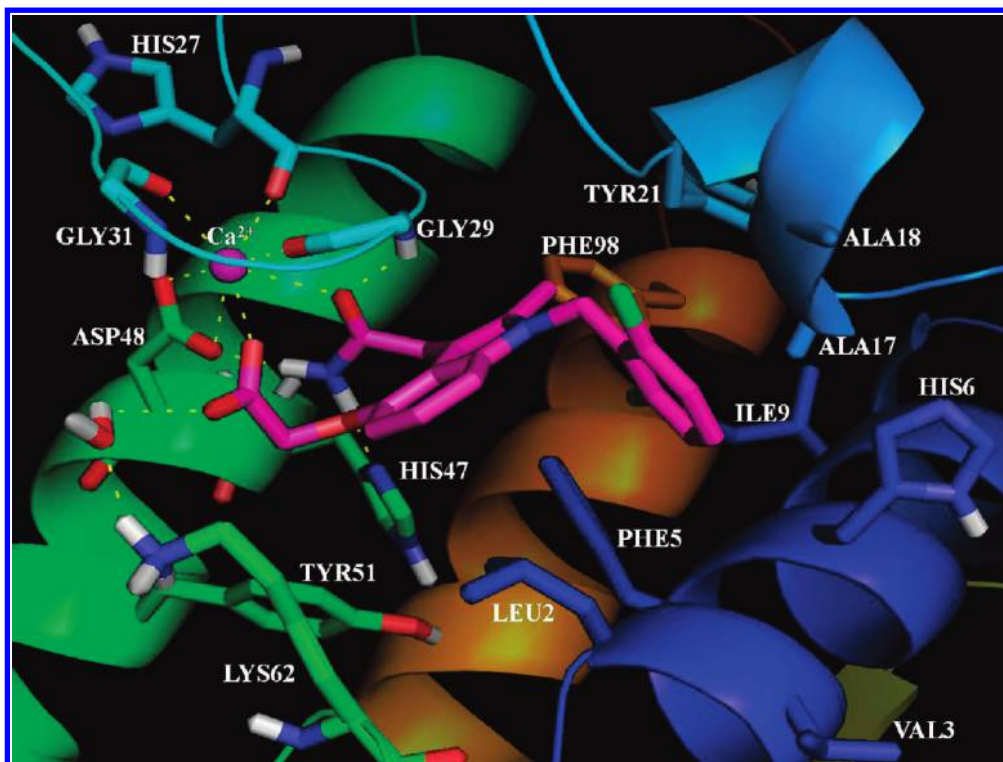


Figure 2. The binding of compound **1** in the active site of the GIIA sPLA₂ enzyme. The enzyme–ligand complex was obtained by automated molecular docking of the indole inhibitor in the enzyme active site using GLIDE.

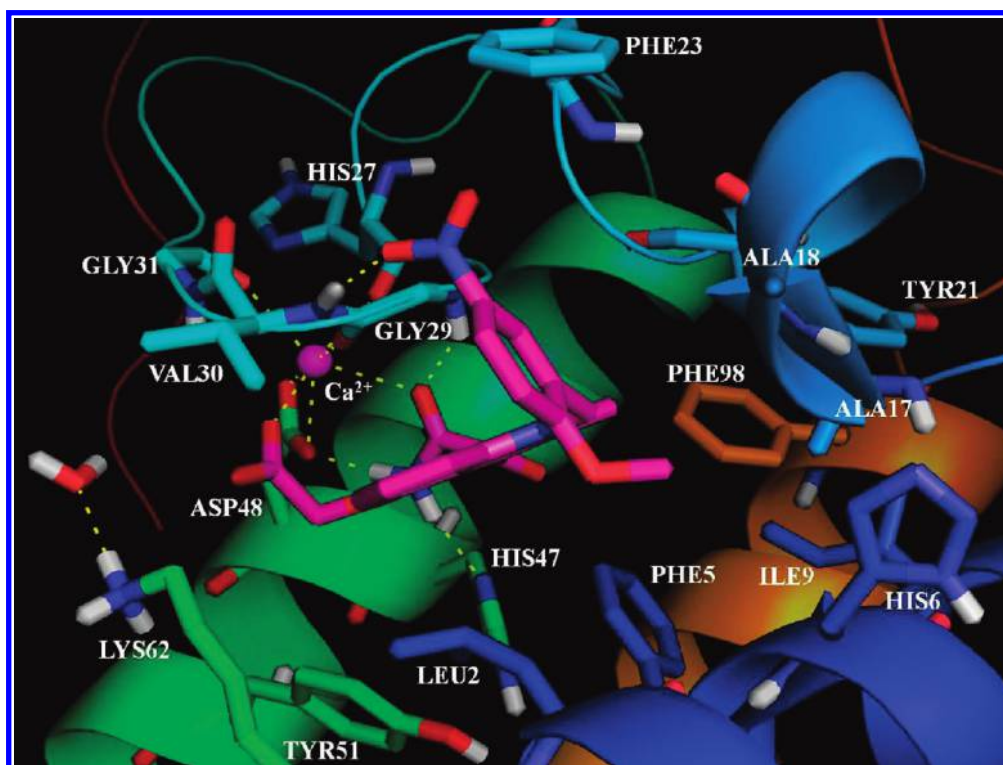


Figure 3. The binding of compound **25** in the active site of the GIIA sPLA₂ enzyme. The enzyme–ligand complex was obtained by automated molecular docking of the indole inhibitor in the enzyme active site using GLIDE.

atom of His47 ($H \cdots N$ 2.00 and $N \cdots N$ 3.00 Å); (iii) one hydrogen bond of one of the hydrogen atoms of the amide group with the oxygen atom of Asp48 ($H \cdots O$ 1.70 and $O \cdots O$ 2.70 Å); and (iv) one hydrogen bond of the oxygen atom of the amide group with the hydrogen atom of the amine group of Gly29 ($O \cdots H-N$ 2.20 and $O \cdots N$ 3.00 Å). Our attention has been focused on understanding the ste-

reoelectronic factors that affect the inhibitory activity of the indole inhibitors. As presented in Figure 3, the methoxy group at the two position of the phenyl ring is bulky enough and cannot be accommodated inside the hydrophobic cavity of the active site. A comparison with the binding of compound **1** reveals that a substituent with the same size as chlorine atom is better for this position. On the other hand,

the nitro group participates in a hydrogen bond with Val30 ($O\cdots H$ 2.20 and $O\cdots N$ 3.20 Å). It seems that this hydrogen bond contributes to lock the phenyl ring in the position presented in Figure 3. As a result, the phenyl ring is not accommodated inside the hydrophobic cavity of the enzyme active site, and it does not participate in aromatic (π - π) stacking interactions or in aromatic/aliphatic interactions with the residues of the hydrophobic region.

By comparing compounds **6** and **28** with compound **1**, it can be concluded that the replacement of the chlorine atom by the bulkier trifluoromethyl group at the two position of the phenyl ring does not affect significantly the inhibitory activity. On the other hand, compound **19** which possesses a nitro group at the three position of the phenyl ring shows almost the half inhibitory activity compared to compound **1**. Another remark can be made for compounds **2–5** and **29** which possess at the three position of the phenyl ring a halogen or a bulky group. These substituents do not decrease significantly the activity compared to compound **1**, as the nitro group does. It seems that the polar nitro group is not an appropriate substituent on the phenyl ring of the indole inhibitors, since it is placed in the hydrophobic region of the enzyme active site. The combination of the nitro group with the bulky methoxy group resulted to the inactivity of compound **25**.

Another remarkable point emerges by comparing compounds **10**, **22**, and **32** with compound **1**. When the substituents on the phenyl ring are very polar groups, the inhibitory activity decreases. In the case of compounds **10** and **22**, the cyano group is a polar substituent and affects negatively the inhibitory activity. Among the two compounds, **22** is less active because the four position of the phenyl ring is directed to the hydrophobic region, but the three position is directed toward the exterior of the enzyme active site (Figure 2). The five fluorine atoms in the case of compound **32** give to the phenyl ring extra polarization, which is not appropriate for the hydrophobic region of the GlIA sPLA₂ enzyme active site.

The comparison of compound **27** with compound **1** indicates that the naphthalene ring may be an appropriate replacement for the phenyl ring. However, the low inhibitory activity of compound **23** reveals that the naphthalene group is not able to accept substituents, because the presence of only one bulky group in the eight position of the naphthalene group decreases the inhibitory activity dramatically. The low inhibitory activity presented by compounds **24**, **26**, and **34** indicates that coumarinyl and phthalimido groups are not suitable replacements for the phenyl ring.

The replacement of the phenyl ring by aliphatic chains (compounds **8**, **15**, **17**, **20**, **21**, **30**, **31**, and **33**) decreases the inhibitory activity in comparison with compound **1**. The phenyl ring is able to participate in aromatic (π - π) stacking interactions, but the aliphatic chain does not. It seems that the phenyl ring itself is essential for the binding. This is validated by the fact that compound **13**, which has only the phenyl ring, has higher inhibitory activity in comparison to compounds having aliphatic chains and possesses almost the same inhibitory activity with compound **8** with the longest aliphatic chain. On the other hand, the increment of the inhibitory activity of compounds **9** and **12** relative to compound **13** shows that a bulky substituent at the four position of the phenyl ring affects positively the inhibitory

Table 2. Statistics and Cross-Validation Results of the CoMFA Model Generated from the Protein-Based Alignment^a

CoMFA model	
PLS components	5
r_{cv}^2	0.793
$r_{\text{training set}}^2$	0.997
SEE	1.847
F	1414.892
electrostatic-steric	0.147:0.853
$r_{\text{bootstrapping}}^2$	0.998 ± 0.001
SEE _{bootstrapping}	1.321 ± 0.982
$r_{\text{test set}}^2$	0.997

^a PLS components: the optimal number of principal components in the PLS model; r_{cv}^2 : the cross-validated correlation coefficient after LOO procedure on the training set of compounds; $r_{\text{training set}}^2$: the correlation coefficient between predicted and experimental values for the training set of compounds; SEE: the standard error of estimate; F: the value of Fisher test; electrostatic-steric: the contribution of the electrostatic and steric fields in the established PLS model; $r_{\text{bootstrapping}}^2$: the average of correlation coefficient for 100 samplings using bootstrapping procedure; SEE_{bootstrapping}: the average standard error of estimate for 100 samplings using bootstrapping procedure; and $r_{\text{test set}}^2$: the correlation coefficient between predicted and experimental values for the test set of compounds.

Table 3. Summary of the Experimental % Inhibition Against the GlIA sPLA₂ Enzyme and the CoMFA-Predicted % Inhibition for the Training and Test Sets of Indole Inhibitors

compound	% inhibition against GlIA sPLA ₂	predicted % inhibition by CoMFA	Δ (exp-pred)
Training Set			
1	100	99.5409	0.4591
2	98	97.5971	0.4029
3	97	94.7576	2.2424
4	96	98.4524	-2.4524
5	95	94.1044	0.8956
6	93	93.8357	-0.8357
7	91	91.8613	-0.8613
8	89	87.8554	1.1446
9	88	89.8195	-1.8195
10	86	85.3116	0.6884
11	84	81.4458	2.5542
12	83	83.6844	-0.6844
13	82	81.3756	0.6244
14	80	84.0841	-4.0841
15	79	79.1629	-0.1629
16	76	74.5003	1.4997
17	64	63.1926	0.8074
18	61	59.3772	1.6228
19	57	59.0770	-2.0770
20	51	48.3345	2.6655
21	39	40.2109	-1.2109
22	29	30.7752	-1.7752
23	24	22.6735	1.3265
24	9	9.9182	-0.9182
25	7	7.7997	-0.7997
26	0	0.7480	-0.7480
Test Set			
27	97	97.1371	-0.1371
28	93	92.6801	0.3199
29	86	86.5151	-0.5151
30	69	66.2000	2.8000
31	57	59.9893	-2.9893
32	33	34.2453	-1.2453
33	22	25.9881	-3.9881
34	2	2.5127	-0.5127

activity. This may be due to the fact that the methyl group can participate in van der Waals contacts with residues, such as Leu2, Val3, and His6, lining the hydrophobic region of

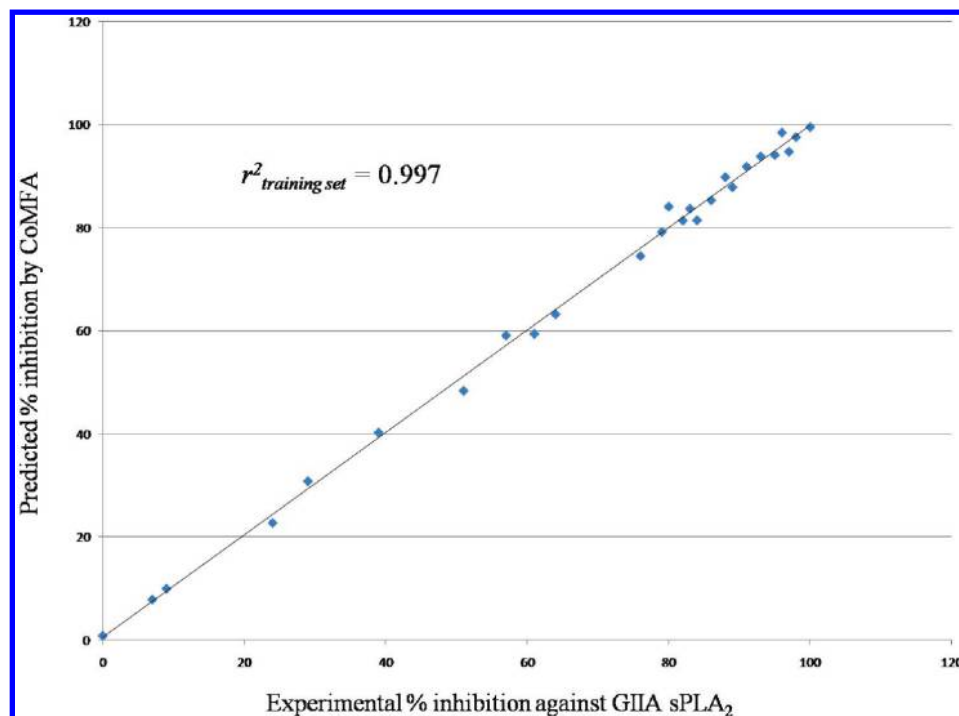


Figure 4. Plot of the experimental % inhibition against the GIIA sPLA₂ enzyme versus the CoMFA-predicted one for the training set of indole inhibitors.

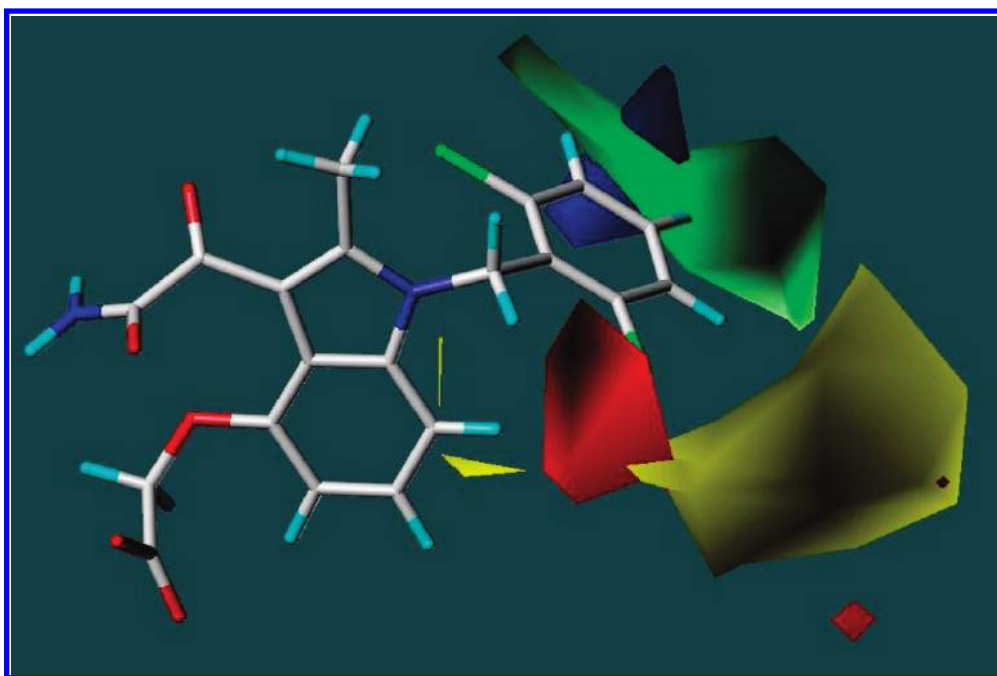


Figure 5. The CoMFA steric and electrostatic fields SD \times coeff contour maps for compound **1**. Bulky groups in the green region favor the inhibitory activity, but bulky groups in the yellow region are not favorable for the inhibitory activity. Negative potentials in the red region favor the inhibitory activity, but negative potentials in the blue region are not desirable.

the enzyme active site (Figure 2). The replacement of the methyl group by the fluorine atom decreases the inhibitor activity (compound **14**) due to the fact that the van der Waals radii of the fluorine atom is smaller than that of the methyl group, and it is not able to participate in very strong van der Waals contacts like the second one. This is also validated by the fact that the replacement of the two chlorine atoms of compound **1** with two fluorine atoms (compounds **7**, **11**, and **16**) decreases the inhibitory activity.

The R group of the indole inhibitors corresponds to a key position for governing the inhibitory activity and especially

the steric effects. The substituents at the benzyl group are important for the inhibitory activity. The question that arises is which combination of these substituents improves the inhibitory activity.

3.2. 3D-QSAR CoMFA Model. The present CoMFA model was generated using a “protein-based” alignment of the 34 indole inhibitors (see Figure 2 in the Supporting Information). The geometries of the inhibitors were determined by their interactions with the GIIA sPLA₂ enzyme active site. For each of the 34 indole inhibitors GLIDE yielded a single conformation, among the several possible

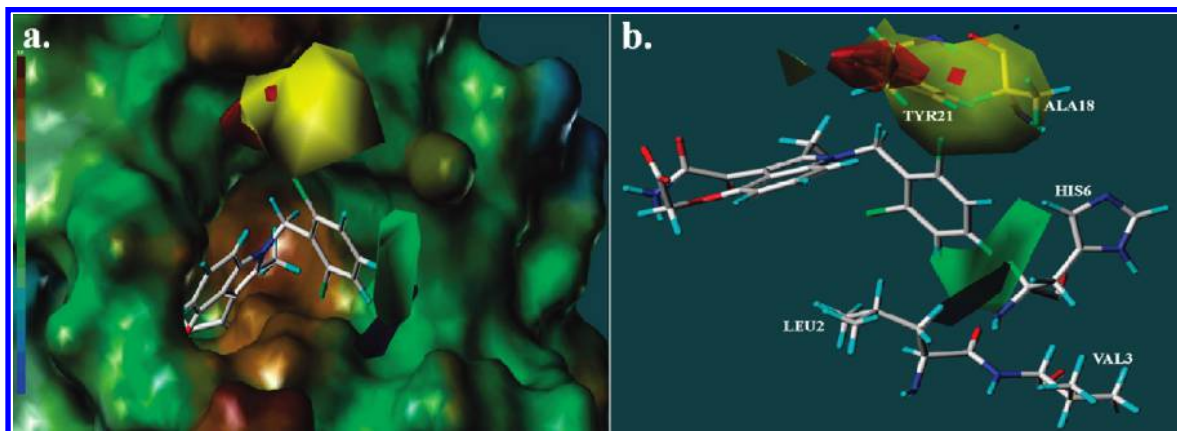


Figure 6. (a) The CoMFA contour maps within the active site of the GIIA sPLA₂ enzyme for compound **1** (MOLCAD lipophilic potential surface was calculated for the receptor with the Connolly method; brown color denotes the most lipophilic areas, and blue color denotes the most hydrophilic areas); and (b) the match of the contour maps with the residues of the GIIA sPLA₂ enzyme active site.

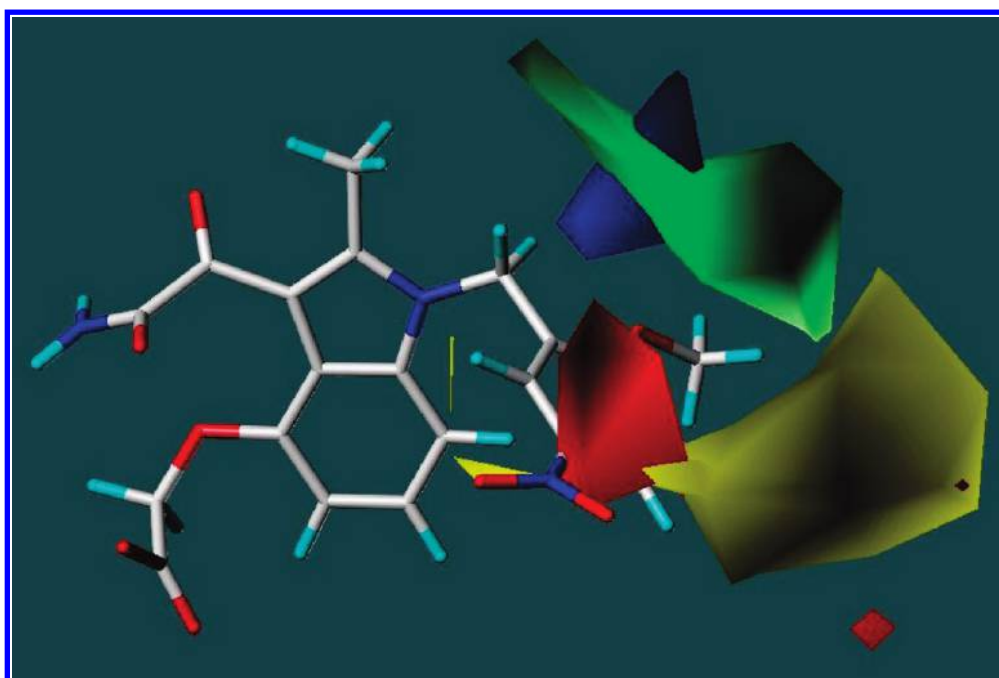


Figure 7. The CoMFA steric and electrostatic fields $SD \times \text{coeff}$ contour maps for compound **25**. Bulky groups in the green region favor the inhibitory activity, but bulky groups in the yellow region are not favorable for the inhibitory activity. Negative potentials in the red region favor the inhibitory activity, but negative potentials in the blue region are not desirable.

low-energy ones derived in the theoretical calculations, for the ligand–enzyme complex.

The predictive ability of the CoMFA model depends on the alignment of the studied compounds. The “protein-based” alignment suggests that the indole inhibitors in the real biological system are aligned in accordance with the ligand–enzyme interactions obtained by the molecular docking using GLIDE. A derived successful CoMFA model suggests the validity of the proposed model of the ligand–enzyme interactions by GLIDE.

The separation of the data set into a training and test set was performed so that the two sets contain a significant diversity of inhibitory activity. Both sets included active and inactive compounds in a range of 0–100% inhibition against the GIIA sPLA₂ enzyme. For better understanding of the stereoelectronic factors underlying the activity, a CoMFA model was generated taking into account both steric and electrostatic fields. The results of this analysis are presented in Table 2, which underlines the contribution of the steric

and electrostatic fields in the CoMFA model. The analysis shows that the relative contributions are 14.7 and 85.3% for the electrostatic and steric fields, respectively. This analysis underlines the important role of CoMFA steric field for the R group of indole inhibitors compared to the electrostatic one. The CoMFA model, in the present study, was used to predict the inhibitory activity for new compounds which potentially can be new GIIA sPLA₂ inhibitors.

A non-cross-validated PLS analysis was performed using the five principal components, which have given the higher cross-validated correlation coefficient after the LOO procedure on the training set of the compounds in order to generate the CoMFA contour maps. This value was selected as the addition of any new component adds less than 5% to the cross-validated correlation coefficient. Table 3 summarizes the experimental and predicted % inhibition and the difference between them. Figure 4 shows the correlation between the experimental and CoMFA-predicted % inhibition values of the non-cross-validated analysis for the training set.

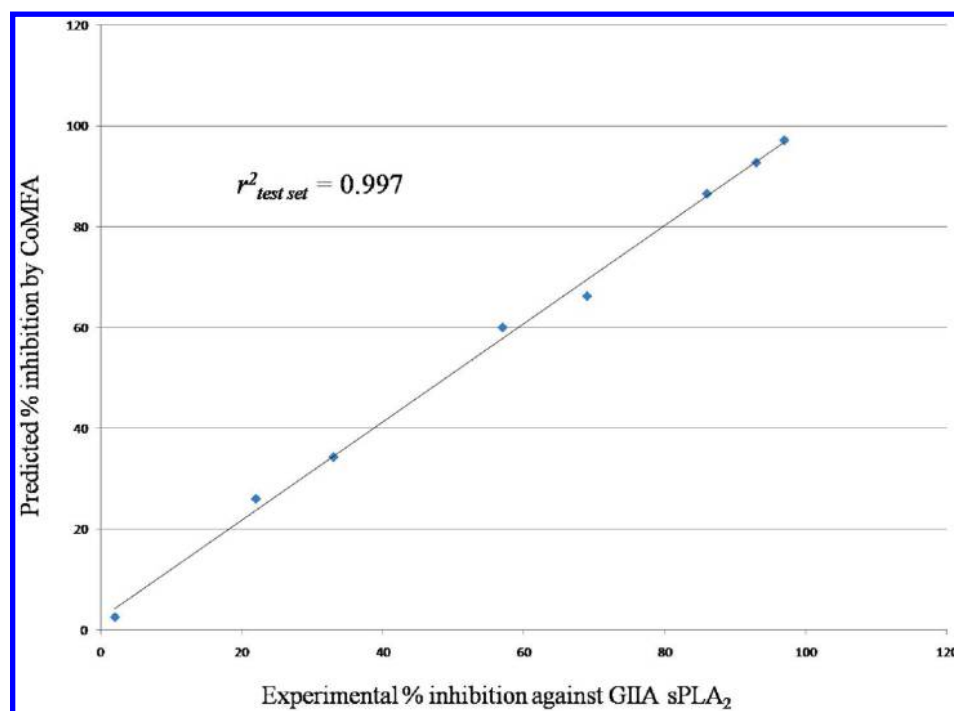
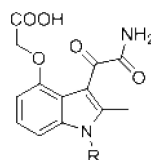


Figure 8. Plot of the experimental % inhibition against the GIIA sPLA₂ enzyme versus the CoMFA-predicted one for the test set of indole inhibitors.

Table 4. Structures Designed Based on the CoMFA Model and Possess Higher Predicted Inhibitory Activity than the Most Active Compound **1**



compound	R group	predicted % inhibition	XP GScore
N1	2,6-Cl ₂ -4-(N ⁺ (CH ₃) ₃)-C ₆ H ₂ CH ₂	119.344	-11.95
N2	2,6-Cl ₂ -4-(CH(CH ₃)(CH ₂ CH ₂ CH ₃))-C ₆ H ₂ CH ₂	117.005	-12.62
N3	2,6-Cl ₂ -4-(CH(CH ₃)(CH ₂ CH ₂ CH ₂ CH ₃))-C ₆ H ₂ CH ₂	116.992	-12.57
N4	2,6-Cl ₂ -4-(CH(CH ₂ CH ₃) ₂)-C ₆ H ₂ CH ₂	116.941	-11.81
N5	2,6-Cl ₂ -4-(CH(CH ₃)(CH ₂ CH ₃))-C ₆ H ₂ CH ₂	116.940	-12.05
N7	2,6-Cl ₂ -4-(SCl ₃)-C ₆ H ₂ CH ₂	116.623	-12.01
N8	2,6-Cl ₂ -4-(OCl ₃)-C ₆ H ₂ CH ₂	115.923	-12.06
N6	2,6-Cl ₂ -4-(CH(CH ₃) ₂)-C ₆ H ₂ CH ₂	115.435	-11.72
N9	2,6-Cl ₂ -4-(CH ₂ CH ₃)-C ₆ H ₂ CH ₂	114.649	-11.62
N10	2,6-Cl ₂ -4-(CH ₂ CH ₂ CH ₃)-C ₆ H ₂ CH ₂	114.642	-11.75
N11	2,6-Cl ₂ -4-(C(CH ₃) ₃)-C ₆ H ₂ CH ₂	113.042	-11.73

The CoMFA contour maps outline a statistic field expressing the relationship between the variation of the steric and electrostatic fields and the variation of the inhibitory activity against the GIIA sPLA₂ enzyme. The values of the fields are calculated at each lattice intersection and are equal to the product descriptor coefficient multiplied by the corresponding standard deviation (SD × coeff). Hence, a low value of SD × coeff indicates that the presence of the corresponding steric or electrostatic field at this point decreases the activity, whereas a high value means that the presence of fragments producing such a field favors the activity. The SD × coeff contour maps for the electrostatic and steric fields are presented in Figure 5 for the more active compound **1**. The contour maps of compound **1** within the MOLCAD surface of the active site are represented in Figure 6a. The MOLCAD surface was developed to display

the lipophilic potential. Figure 6b represents the match of the contour maps with the residues of the GIIA sPLA₂ enzyme.

Compounds **1** (Figure 5) and **25** (Figure 7) illustrate the main features of the CoMFA contour maps. The colored regions on the contour maps mark the favorable and unfavorable characteristics that should have the substituents on the phenyl ring. In Figure 5, the hydrogen atom at the four position of the phenyl ring is extended near the green region, which means that bulky groups are desirable and affect the inhibitory activity in a favorable way. The green contour around the hydrogen atom at the four position of the phenyl ring approaches the lipophilic region (Figure 6a) near Leu2, Val3, and His6 (Figure 6b), suggesting that a bulkier group will increase the inhibitory activity, an observation that is in agreement with the CoMFA model. Near the green region, there is a blue region which indicates that negative potentials are not desirable and affect the inhibitory activity in an unfavorable way. The position two of the phenyl ring is extended near a yellow region indicating that the bulky groups are not desirable and affect also the inhibitory activity in an unfavorable way. The yellow contour is on the lipophilic region of the active site (Figure 6a), suggesting that bulkier groups at this position will clash with the residues, such as Ala18 and Tyr21 (Figure 6b). Near the yellow region there is a red region which shows that negative potentials are desirable for the inhibitory activity. The chlorine atom seems to have the suitable properties for this region because it is not as bulky to approach the yellow contour region, but it has enough size to approach the red contour region. By examining the position of compound **25** in the contour maps, it is possible to understand why this inhibitor is inactive. The positively charged nitrogen atom of the nitro group at the five position of the phenyl ring is in vicinity with the red contour region, and the methoxy group at the two position of the phenyl ring is in spatial

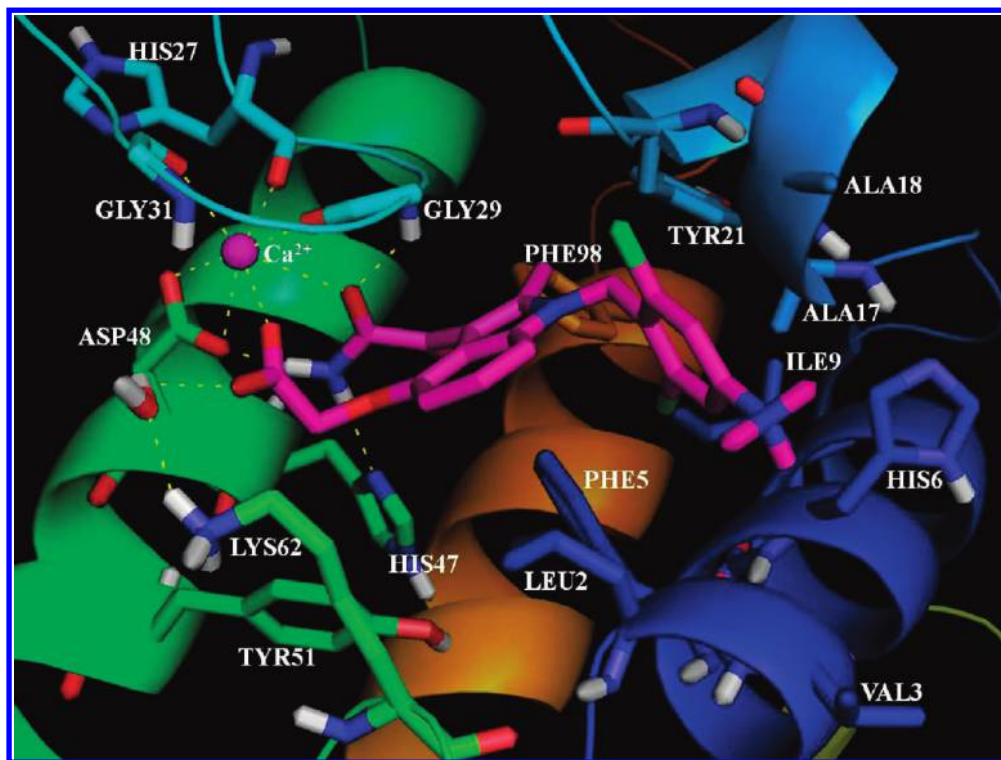


Figure 9. The binding of compound **N1** in the active site of the GIIA sPLA₂ enzyme. The enzyme–ligand complex was obtained by automated molecular docking of the compound in the enzyme active site using GLIDE.

proximity to the yellow contour region. Thus, the two groups are characterized by unfavorable interactions. This is in accordance with the molecular docking calculations in which compound **25** indicates low XP binding score.

3.3. Validation of the CoMFA Model. To further assess the robustness and statistical confidence of the generated CoMFA model bootstrapping analysis for 100 runs was performed (Table 2). The higher value of $r^2_{\text{bootstrapping}}$ ($r^2_{\text{bootstrapping}} = 0.998 \pm 0.001$) indicates the robustness and statistical confidence of the generated CoMFA model.

The sensitivity of the CoMFA results toward the training set selection has been also examined by repeating the analysis on the training set with different ligand partitioning on the ligand set. The r^2_{cv} values range between 0.767–0.792, confirming the LOO results on the first partition and the stability of the CoMFA model.

To further validate the stability and predictive ability of the CoMFA model, eight compounds not included in the training set were used as a test set. The predicted results for the test set are listed in Table 3. Figure 8 indicates that the predicted values of % inhibition by the CoMFA model are in agreement with the experimental ones in a tolerable error range with $r^2_{\text{test set}} = 0.997$.

The conclusion derived from the validation part of this study is that the CoMFA model could be used reliably to design new inhibitors with improved inhibitory activity against the GIIA sPLA₂ enzyme. The tight correlation between experimentally observed and predicted values in this study suggests that the present model is able to provide reliable predictions of GIIA sPLA₂ inhibitory capacities in a set of new inhibitors.

3.4. Design of New Indole Inhibitors. According to the detailed contour analyses of the CoMFA model, useful information on the structural requirements for the observed

inhibitory activities is obtained. We have employed this information to design several analogues showing improved inhibitory activity. The most potent molecule (compound **1**) was used as a reference structure to design new molecules.

Initially, the two chlorine atoms at the positions two and six of the phenyl ring were replaced with the fluorine, bromine, and iodine atoms. The predicted inhibitory activities for these compounds were lower than the inhibitory activity of compound **1**. Chlorine atom is the best substituent for these positions and especially for the position two, which is in spatial vicinity with the red and yellow contours (Figure 5). Substituents at the five position of the phenyl ring do not affect significantly the predicted inhibitory activity. The three position approaches the yellow contour, and substituents bulkier than the hydrogen atom may contribute to the decrease of the inhibitory activity. The new analogues that indicated higher predicted inhibitory activity than compound **1** are listed in Table 4. The changes on the new designed compounds have been made at the four position of the phenyl ring. The % inhibitory activity in the *in vitro* test was measured using ligand concentration 0.33 μM .⁴⁰ The % inhibitory activity higher than 100, calculated for the new compounds, means that the new compounds might present 100% inhibitory activity against the GIIA sPLA₂ enzyme at a lower concentration than 0.33 μM .

The new designed compounds have been subsequently docked in the GIIA sPLA₂ enzyme active site in order to see how the substituent at the four position of the phenyl ring interacts with the enzyme active site. The XP binding scores calculated for the compounds (Table 4) are higher than the one of the template compound **1** (Table 1). The binding of these compounds is very similar with the binding of compound **1** and also with each other. The binding of compound **N1** is presented in Figure 9 (for the binding of

compounds **N2** and **N3** see Figure 4 and Figure 5 in the Supporting Information). The polar interactions shown in compound **N1** are identical to those shown in compound **1** and are the same for all the compounds in Table 4. The phenyl ring of the new compounds orients in a similar way in the active site as the phenyl ring of compound **1** and participates in aromatic (π - π) stacking interactions with the residues Phe5 and His6. The indole ring participates in aromatic (π - π) stacking interactions with residues Phe5 and His47. The substituent at the four position of the phenyl ring of compound **N1** participates in van der Waals contacts with the residues Leu2, Val3, and His6 (Figure 9) and might be the reason that the XP binding score is increased, in comparison with the XP binding score of compound **1**. The substituent at the four position of the phenyl ring accommodated at the same hydrophobic region in all the new designed compounds and interacts with the residues Leu2, Val3, and His6.

4. CONCLUSION

A combination of automated docking calculations and three-dimensional quantitative structure-activity relationship studies using the comparative molecular field analysis method (3D-QSAR CoMFA) was performed on a set of 34 GIIA secreted phospholipase A₂ (GIIA sPLA₂) indole inhibitors for designing new compounds with improved inhibitory activity. The docking of two crystallographic indole inhibitors in the enzyme active site using GLIDE showed that the algorithm can reproduce experimental crystallographic data, and thus a reliable docking was performed for all the 34 indole inhibitors which have been studied using the extra-precision (XP) mode.

The binding of the crystallographic compounds, after their molecular docking with GLIDE, revealed three new hydrogen bonds with the residues Gly29, Gly31, and His47. The XP binding scores calculated by the molecular docking of the 34 indole inhibitors with GLIDE were compared with their experimental inhibitory activity against the GIIA sPLA₂ enzyme. The linearity of the plot ($r^2 = 0.666$, $N = 34$) presents a good correlation between the XP binding scores and the experimental inhibitory activity of the indole inhibitors.

The best score docking pose for each indole inhibitor was then used to generate the CoMFA model. The data set of the 34 compounds was divided into two subsets, one with 26 compounds to construct the CoMFA model (training set) and the other with 8 compounds for the validation of the model (test set). The CoMFA model was created using a "protein-based" alignment, and according to the cross-validation test ($r_{cv}^2 = 0.793$) has a good predictive capacity. The robustness and the statistic confidence of the generated CoMFA model ($r_{bootstrapping}^2 = 0.998 \pm 0.001$) and its predictive ability ($r_{test\ set}^2 = 0.997$) have shown that the model can be used to design new compounds and further evaluate how the structural changes affect the inhibitory activity.

This robust and predictive model was then used to design new compounds presenting improved inhibitory activity. The new compounds were subsequently docked in the GIIA sPLA₂ enzyme active site to check how they interact with the enzyme active site. The combination of the molecular docking calculations and the three-dimensional QSAR

CoMFA studies gave important information about the binding of the 34 indole inhibitors and the structural changes that affect the inhibitory activity of these compounds against the GIIA sPLA₂ enzyme. This model can be used to guide the rational design of new compounds presenting improved inhibitory activity against the GIIA sPLA₂ enzyme.

ACKNOWLEDGMENT

This work was supported in part by the University of Athens (ELKE).

Supporting Information Available: Superimposition of the four crystal structures of the GIIA sPLA₂ enzyme, alignment of the data set used in the 3D-QSAR CoMFA model, and binding of the crystallographic inhibitors indole8 and indole6. This material is available free of charge via the Internet at <http://pubs.acs.org>.

REFERENCES AND NOTES

- (1) Burke, J. E.; Dennis, E. A. Phospholipase A₂ biochemistry. *Cardiovasc. Drugs Ther.* **2009**, *23*, 49–59.
- (2) Schaloske, R. H.; Dennis, E. A. The phospholipase A₂ superfamily and its group numbering system. *Biochim. Biophys. Acta* **2006**, *1761*, 1246–59.
- (3) Funk, C. D. Prostaglandins and leukotrienes: advances in eicosanoid biology. *Science* **2001**, *294*, 1871–5.
- (4) Kudo, I.; Murakami, M. Phospholipase A₂ enzymes. *Prostaglandins Other Lipid Mediators* **2002**, *68–69*, 3–58.
- (5) Oestvang, J.; Johansen, B. Phospholipase A₂: a key regulator of inflammatory signalling and a connector to fibrosis development in atherosclerosis. *Biochim. Biophys. Acta* **2006**, *1761*, 1309–16.
- (6) Back, M. Leukotriene signaling in atherosclerosis and ischemia. *Cardiovasc. Drugs Ther.* **2009**, *23*, 41–8.
- (7) Moolenaar, W. H.; van Meeteren, L. A.; Giepmans, B. N. The ins and outs of lysophosphatidic acid signaling. *Bioessays* **2004**, *26*, 870–81.
- (8) Gelb, M. H.; Min, J. H.; Jain, M. K. Do membrane-bound enzymes access their substrates from the membrane or aqueous phase: interfacial versus non-interfacial enzymes. *Biochim. Biophys. Acta* **2000**, *1488*, 20–7.
- (9) Zhou, L.; Fang, C.; Wei, P.; Liu, S.; Liu, Y.; Lai, L. Chemically induced dimerization of human nonpancreatic secretory phospholipase A₂ by bis-indole derivatives. *J. Med. Chem.* **2008**, *51*, 3360–6.
- (10) Gelb, M. H.; Jain, M. K.; Hanel, A. M.; Berg, O. G. Interfacial enzymology of glycerolipid hydrolases: lessons from secreted phospholipases A₂. *Annu. Rev. Biochem.* **1995**, *64*, 653–88.
- (11) Lambeau, G.; Gelb, M. H. Biochemistry and physiology of mammalian secreted phospholipases A₂. *Annu. Rev. Biochem.* **2008**, *77*, 495–520.
- (12) Boyanovsky, B. B.; Webb, N. R. Biology of secretory phospholipase A₂. *Cardiovasc. Drugs Ther.* **2009**, *23*, 61–72.
- (13) Winget, J. M.; Pan, Y. H.; Bahnson, B. J. The interfacial binding surface of phospholipase A₂s. *Biochim. Biophys. Acta* **2006**, *1761*, 1260–9.
- (14) Gelb, M. H.; Valentin, E.; Ghomashchi, F.; Lazdunski, M.; Lambeau, G. Cloning and recombinant expression of a structurally novel human secreted phospholipase A₂. *J. Biol. Chem.* **2000**, *275*, 39823–6.
- (15) Valentin, E.; Lambeau, G. Increasing molecular diversity of secreted phospholipases A₂ and their receptors and binding proteins. *Biochim. Biophys. Acta* **2000**, *1488*, 59–70.
- (16) Kramer, R. M.; Hession, C.; Johansen, B.; Hayes, G.; McGray, P.; Chow, E. P.; Tizard, R.; Pepinsky, R. B. Structure and properties of a human non-pancreatic phospholipase A₂. *J. Biol. Chem.* **1989**, *264*, 5768–75.
- (17) Seilhamer, J. J.; Pruzanski, W.; Vadas, P.; Plant, S.; Miller, J. A.; Kloss, J.; Johnson, L. K. Cloning and recombinant expression of phospholipase A₂ present in rheumatoid arthritic synovial fluid. *J. Biol. Chem.* **1989**, *264*, 5335–8.
- (18) Valentin, E.; Ghomashchi, F.; Gelb, M. H.; Lazdunski, M.; Lambeau, G. On the diversity of secreted phospholipases A₂. Cloning, tissue distribution, and functional expression of two novel mouse group II enzymes. *J. Biol. Chem.* **1999**, *274*, 31195–202.
- (19) Dennis, E. A. Diversity of group types, regulation, and function of phospholipase A₂. *J. Biol. Chem.* **1994**, *269*, 13057–60.

- (20) Scott, D. L.; White, S. P.; Otwinowski, Z.; Yuan, W.; Gelb, M. H.; Sigler, P. B. Interfacial catalysis: the mechanism of phospholipase A₂. *Science* **1990**, *250*, 1541–6.
- (21) Scott, D. L.; White, S. P.; Browning, J. L.; Rosa, J. J.; Gelb, M. H.; Sigler, P. B. Structures of free and inhibited human secretory phospholipase A₂ from inflammatory exudate. *Science* **1991**, *254*, 1007–10.
- (22) Wery, J. P.; Schevitz, R. W.; Clawson, D. K.; Bobbitt, J. L.; Dow, E. R.; Gamboa, G.; Goodson, T., Jr.; Hermann, R. B.; Kramer, R. M.; McClure, D. B.; Mihelich, E. D.; Putnam, J. E.; Sharp, J. D.; Stark, D. H.; Teater, C.; Warrick, M. W.; Jones, N. D. Structure of recombinant human rheumatoid arthritic synovial fluid phospholipase A₂ at 2.2 Å resolution. *Nature* **1991**, *352*, 79–82.
- (23) Mouchlis, V. D.; Mavromoustakos, T. M.; Kokotos, G. Design of new secreted phospholipase A₂ inhibitors based on docking calculations by modifying the pharmacophore segments of the FPL67047XX inhibitor. *J. Comput.-Aided Mol. Des.* **2010**, *24*, 107–15.
- (24) Li, B.; Liu, Z.; Zhang, L. Multiple-docking and affinity fingerprint methods for protein classification and inhibitors selection. *J. Chem. Inf. Model.* **2009**, *49*, 1725–33.
- (25) Tomoo, K.; Yamane, A.; Ishida, T.; Fujii, S.; Ikeda, K.; Iwama, S.; Katsumura, S.; Sumiya, S.; Miyagawa, H.; Kitamura, K. X-ray crystal structure determination and molecular dynamics simulation of phospholipase A₂ inhibited by amide-type substrate analogues. *Biochim. Biophys. Acta* **1997**, *1340*, 178–86.
- (26) Hariprasad, V.; Kulkarni, V. M. A molecular dynamics study of the three-dimensional model of human synovial fluid phospholipase A₂-transition state mimic complexes. *J. Mol. Recognit.* **1996**, *9*, 95–102.
- (27) Ortiz, A. R.; Pastor, M.; Palomer, A.; Cruciani, G.; Gago, F.; Wade, R. C. Reliability of comparative molecular field analysis models: effects of data scaling and variable selection using a set of human synovial fluid phospholipase A₂ inhibitors. *J. Med. Chem.* **1997**, *40*, 1136–48.
- (28) Ortiz, A. R.; Pisabarro, M. T.; Gago, F.; Wade, R. C. Prediction of drug binding affinities by comparative binding energy analysis. *J. Med. Chem.* **1995**, *38*, 2681–91.
- (29) Magrioti, V.; Kokotos, G. Phospholipase A₂ inhibitors as potential therapeutic agents for the treatment of inflammatory diseases. *Expert Opin. Ther. Pat.* **2010**, *20*, 1–18.
- (30) Garcia-Garcia, H. M.; Serruys, P. W. Phospholipase A₂ inhibitors. *Curr. Opin. Lipidol.* **2009**, *20*, 327–332.
- (31) Magrioti, V.; Kokotos, G. Synthetic Inhibitors of Group IVA and Group VIA Phospholipase A₂. *Curr. Med. Chem.: Anti-Inflammatory Anti-Allergy Agents* **2006**, *5*, 189–203.
- (32) Reid, R. C. Inhibitors of secretory phospholipase A₂ group IIA. *Curr. Med. Chem.* **2005**, *12*, 3011–26.
- (33) Meyer, M. C.; Rastogi, P.; Beckett, C. S.; McHowat, J. Phospholipase A₂ inhibitors as potential anti-inflammatory agents. *Curr. Pharm. Des.* **2005**, *11*, 1301–12.
- (34) Kuntz, I. D.; Meng, E. C.; Shoichet, B. K. Structure-Based Molecular Design. *Acc. Chem. Res.* **2002**, *27*, 117–123.
- (35) Tuccinardi, T. Docking-based virtual screening: recent developments. *Comb. Chem. High Throughput Screening* **2009**, *12*, 303–14.
- (36) Halperin, I.; Ma, B.; Wolfson, H.; Nussinov, R. Principles of docking: An overview of search algorithms and a guide to scoring functions. *Proteins* **2002**, *47*, 409–43.
- (37) Taylor, R. D.; Jewsbury, P. J.; Essex, J. W. A review of protein-small molecule docking methods. *J. Comput.-Aided Mol. Des.* **2002**, *16*, 151–66.
- (38) Kauvar, L. M.; Higgins, D. L.; Villar, H. O.; Sportsman, J. R.; Engqvist-Goldstein, A.; Bukar, R.; Bauer, K. E.; Dilley, H.; Rocke, D. M. Predicting ligand binding to proteins by affinity fingerprinting. *Chem. Biol.* **1995**, *2*, 107–18.
- (39) Cramer III, R. D.; Patterson, D. E.; Bunce, J. D. Comparative molecular field analysis (CoMFA). 1. Effect of shape on binding of steroids to carrier proteins. *J. Am. Chem. Soc.* **1988**, *110*, 5959–5967.
- (40) Smart, B. P.; Pan, Y. H.; Weeks, A. K.; Bollinger, J. G.; Bahnsen, B. J.; Gelb, M. H. Inhibition of the complete set of mammalian secreted phospholipases A₂ by indole analogues: a structure-guided study. *Bioorg. Med. Chem.* **2004**, *12*, 1737–49.
- (41) *Glide*, version 5.5; Schrödinger, LLC: New York, 2009.
- (42) Friesner, R. A.; Banks, J. L.; Murphy, R. B.; Halgren, T. A.; Klicic, J. J.; Mainz, D. T.; Repasky, M. P.; Knoll, E. H.; Shelley, M.; Perry, J. K.; Shaw, D. E.; Francis, P.; Shenkin, P. S. *Glide*: a new approach for rapid, accurate docking and scoring. 1. Method and assessment of docking accuracy. *J. Med. Chem.* **2004**, *47*, 1739–49.
- (43) Halgren, T. A.; Murphy, R. B.; Friesner, R. A.; Beard, H. S.; Frye, L. L.; Pollard, W. T.; Banks, J. L. *Glide*: a new approach for rapid, accurate docking and scoring. 2. Enrichment factors in database screening. *J. Med. Chem.* **2004**, *47*, 1750–9.
- (44) Friesner, R. A.; Murphy, R. B.; Repasky, M. P.; Frye, L. L.; Greenwood, J. R.; Halgren, T. A.; Sanschagrin, P. C.; Mainz, D. T. Extra precision glide: docking and scoring incorporating a model of hydrophobic enclosure for protein-ligand complexes. *J. Med. Chem.* **2006**, *49*, 6177–96.
- (45) Schevitz, R. W.; Bach, N. J.; Carlson, D. G.; Chirgadze, N. Y.; Clawson, D. K.; Dillard, R. D.; Draheim, S. E.; Hartley, L. W.; Jones, N. D.; Mihelich, E. D.; Olkowski, J. L.; Snyder, D. W.; Sommers, C.; Wery, J.-P. Structure-based design of the first potent and selective inhibitor of human non-pancreatic secretory phospholipase A₂. *Nat. Struct. Biol.* **1995**, *2*, 458–65.
- (46) Cha, S. S.; Lee, D.; Adams, J.; Kurdyla, J. T.; Jones, C. S.; Marshall, L. A.; Bolognese, B.; Abdel-Meguid, S. S.; Oh, B. H. High-resolution X-ray crystallography reveals precise binding interactions between human nonpancreatic secreted phospholipase A₂ and a highly potent inhibitor (FPL67047XX). *J. Med. Chem.* **1996**, *39*, 3878–81.
- (47) Hansford, K. A.; Reid, R. C.; Clark, C. I.; Tyndall, J. D. A.; Whitehouse, M. W.; Guthrie, T.; McGeary, R. P.; Schafer, K.; Martin, J. L.; Fairlie, D. P. D-Tyrosine as a chiral precursor to potent inhibitors of human nonpancreatic secretory phospholipase A₂ (IIa) with anti-inflammatory activity. *ChemBioChem* **2003**, *4*, 181–185.
- (48) *Maestro*, version 9.0; Schrödinger, LLC: New York, 2009.
- (49) *Schrödinger Suite 2009 Protein Preparation Wizard*, Epik version 2.0, Impact version 5.5, Prime version 2.1; Schrödinger, LLC: New York, 2009.
- (50) *Epik*, version 2.0; Schrödinger, LLC: New York, 2009.
- (51) Shelley, J. C.; Cholleti, A.; Frye, L. L.; Greenwood, J. R.; Timlin, M. R.; Uchimaya, M. Epik: a software program for pKa prediction and protonation state generation for drug-like molecules. *J. Comput.-Aided Mol. Des.* **2007**, *21*, 681–91.
- (52) *MacroModel*, version 9.7; Schrödinger, LLC: New York, 2009.
- (53) Kaminski, G. A.; Friesner, R. A.; Tirado-Rives, J.; Jorgensen, W. L. Evaluation and reparametrization of the OPLS-AA force field for proteins via comparison with accurate quantum chemical calculations on peptides. *J. Phys. Chem. B* **2001**, *105*, 6474–6487.
- (54) Polak, E.; Ribiere, G. Note sur la convergence de méthodes de directions conjuguées. *Rev. Fr. Informat. Recherche Operationelle Ser. Rouge* **1969**, *16*, 35–43.
- (55) Still, W. C.; Tempczyk, A.; Hawley, R. C.; Hendrickson, T. Semi-analytical treatment of solvation for molecular mechanics and dynamics. *J. Am. Chem. Soc.* **1990**, *112*, 6127–6129.
- (56) *LigPrep*, version 2.3; Schrödinger, LLC: New York, 2009.
- (57) Eldridge, M. D.; Murray, C. W.; Auton, T. R.; Paolini, G. V.; Mee, R. P. Empirical scoring functions: I. The development of a fast empirical scoring function to estimate the binding affinity of ligands in receptor complexes. *J. Comput.-Aided Mol. Des.* **1997**, *11*, 425–45.
- (58) Gasteiger, J.; Marsili, M. Iterative partial equalization of orbital electronegativity—a rapid access to atomic charges. *Tetrahedron* **1980**, *36*, 3219–3228.
- (59) Purcell, W. P.; Singer, J. A. A brief review and table of semiempirical parameters used in the Hückel molecular orbital method. *J. Chem. Eng. Data* **1967**, *12*, 235–246.
- (60) *SYBYL/QSAR and COMFA*, version 8.0; Tripos Inc.: St. Louis, MO, 2007.
- (61) Clark, M.; Cramer, D. R., III; Van Opdenbosch, N. Validation of the general purpose tripos 5.2 force field. *J. Comput. Chem.* **1989**, *10*, 982–1012.
- (62) Stone, M. Cross-validatory choice and assessment of statistical predictions. *J. Roy. Stat. Soc. B Stat. Meth.* **1974**, *36*, 111–147.
- (63) Cramer, R. D., III; Bunce, J. D.; Patterson, D. E.; Frank, I. E. Crossvalidation, bootstrapping, and partial least squares compared with multiple regression in conventional QSAR Studies. *Quant. Struct.-Act. Relat.* **1988**, *7*, 18–25.
- (64) Shao, J. Bootstrap model selection. *J. Am. Stat. Assoc.* **1996**, *91*, 655–665.
- (65) Burley, S. K.; Petsko, G. A. Aromatic-aromatic interaction: a mechanism of protein structure stabilization. *Science* **1985**, *229*, 23–8.
- (66) Hunter, C. A.; Singh, J.; Thornton, J. M. Pi-pi interactions: the geometry and energetics of phenylalanine-phenylalanine interactions in proteins. *J. Mol. Biol.* **1991**, *218*, 837–46.